Struct Multidisc Optim (2016) 54:1573–1585
DOI 10.1007/s00158-016-1545-8

INDUSTRIAL APPLICATION

Statistical calibration and validation of elasto-plastic insertion analysis in pyrotechnically actuated devices

Hee-Seong Kim[1] · **Seung-Gyo Jang**[2] · **Nam-Ho Kim**[3] · **Joo-Ho Choi**[4]

Received: 15 January 2016 / Revised: 16 July 2016 / Accepted: 20 July 2016 / Published online: 19 August 2016

Abstract A statistical procedure for calibration and validation is addressed as an industrial application for the analysis problem of piston insertion into the housing in the pyrotechnically actuated device. Three parameters are identified in the model that affect the solution greatly but they are not known a priori. Bayesian approach is employed to calibrate these parameters in the form of distributions, which account for the uncertainty of the model and test data. In order to validate the model, similar new problems are introduced, analyzed and tested for validation purpose. As a result, the predictions in the new problems are found to work equally well as in the calibration problem, which suggests that it is useful in the subsequent new design without additional test procedure.

Keywords Statistical uncertainty · Elasto-plastic insertion · Calibration · Validation · Bayesian approach · Markov Chain Monte Carlo

✉ Joo-Ho Choi
jhchoi@kau.ac.kr

[1] Department of Aerospace & Mechanical Engineering, Korea Aerospace University, Goyang-City, Gyeonggi-do, South Korea

[2] Advanced Propulsion Technology Center, Agency for Defense Development, Daejon, South Korea

[3] Department, Mechanical & Aerospace Engineering, University of Florida, Gainseville, FL, USA

[4] School of Aerospace & Mechanical Engineering, Korea Aerospace University, Goyang-City, Gyeonggi-do, South Korea

1 Introduction

A Pyrotechnically Actuated Device (PAD) performs critical functions for aerospace and defense systems such as stage separation, wing deployment and propulsion control. There are many different PADs such as pin-puller, cable cutter, pyro-valve and so on. Among those, pyro-valve is considered in this study, which consists of pyrotechnic pressure chamber, piston and housing as illustrated in Fig. 1. The role of the valve is to open a gas or liquid flow. By combustion of a self-contained energy source in the pyrotechnic chamber, pressure is generated to insert piston into the housing and triggers intended mission. The housing is designed to absorb the kinetic energy of piston and prevent bouncing back by introducing interference between the piston and housing. Due to its critical mission in the aerospace and defense system, very high reliability is required but the evaluation is difficult because it is single use device. Too weak pyrotechnics or too much interference may cause failure of the piston to reach the end and mission abort. As the number of tests are limited due to the single use nature, modeling and simulation is useful to assess the reliability of current design and new development. The whole computational model requires complicated time-dependent analysis including the burning of solid explosive to form gas within the actuator, expansion of the gas to the chamber, and insertion of the piston into the housing by gas pressure. The coupling of combustion energy to piston–housing deformation by the gas pressure is also necessary. Few literatures are available on this analysis, with the application to a couple of variants such as pyro-valve (Braud et al. 2007; Paul and Gonthier 2010) and pin puller (Jones et al.

1994). In their analyses, comprehensive mathematical model was formulated by coupling the explosive combustion, pressure generation and piston-housing deformation. As a result, a set of one-dimensional equations are developed to determine the pressure history and piston displacement during the operation. A closed form elasto-plastic solution is incorporated for the piston insertion into the housing by assuming them as a series of thin disks with interference fit and their material behavior as linear strain hardening. While the mathematical model approach facilitates extensive parametric study with convenience, its value is limited due to the lack of reality.

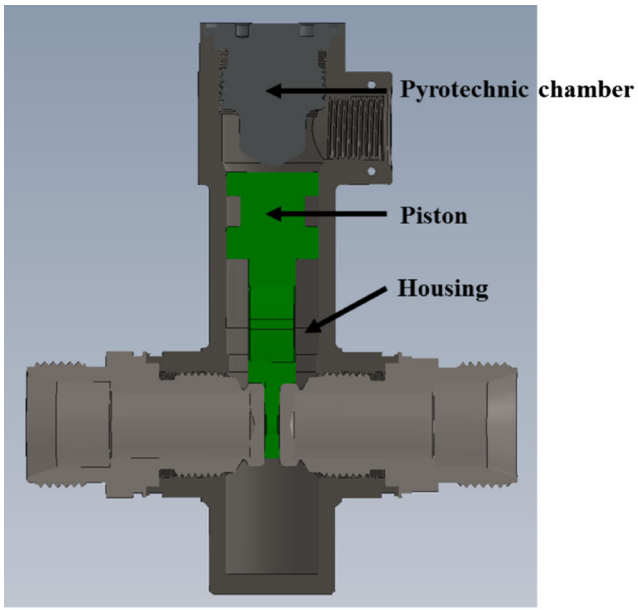

(a) cross section view at initial setup

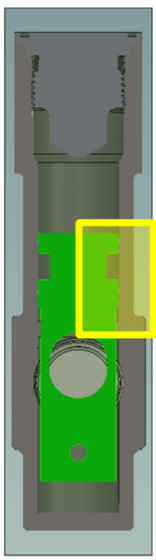

(b) side view after the operation

Fig. 1 Cross section and side view of pyro-valve

In this study, we focus on the elasto-plastic piston-housing deformation which is one of the important parts of the whole computational model. Inaccurate analysis of this may lead to the insufficient insertion or excessive deformation of the piston into the housing leading to catastrophic failure. The deformation is investigated in more realistic manner by employing the finite element software ANSYS to analyze the contact and nonlinear material behavior during the insertion. Although the deformation takes place instantaneously within a fraction of second, the process can be assumed as quasi static because the influence of the inertia to the stress is marginal as was mentioned in (Braud et al. 2007). For this purpose, an interested part given by the rectangle of Fig. 1b is considered to conduct the quasi-static elasto-plastic analysis during the piston insertion into the housing. The finite element model, however, has still inaccuracy problems that limits its use in practice: the finite element analysis (FEA) model has errors due to modeling only an interested part of the whole structure, and usually some unknown input parameters exist in the model. Typical resolution is to conduct real test and determine unknown parameters of the model to match with the actual test data, which is known as model calibration. In traditional approach, the calibration process has been explored in a deterministic sense without accounting for the uncertainties of the modeling inaccuracy, measurement errors and insufficient test data, which may lead to wrong conclusions. In order to account for these uncertainties, statistical approach has been studied by a number of literatures. In a fundamental work, Kennedy and O'Hagan (2001) proposed a comprehensive formulation with the title of Bayesian calibration, which was followed by many other groups (e.g., Higdon et al. 2004; Bayarri et al. 2012). If we restrict the literature to the material parameters identification, numerous papers are still available that have addressed Bayesian calibration. Only a few are referenced in this paper to illustrate the applications. Marwala et al. (2005) applied the method to the finite element model updating in the frequency response analysis of the aluminum beam. Gang et al. (2012) estimated unknown parameters of alloy material in their viscoplastic model of solder joint analysis. Sankararaman et al. (2011) presented a method for calibration and validation of fatigue crack growth model and applied to the surface cracking of a cylindrical component. Straub and Papaioannou (2014) have proposed structural reliability methods to improve MCMC sampling and applied to the parameter identification in a dynamic system and Bayesian updating of a random field of a geotechnical site.

In the Bayesian calibration approach, it is common to employ Gaussian stochastic model to approximate the original computer model as well as its bias from the

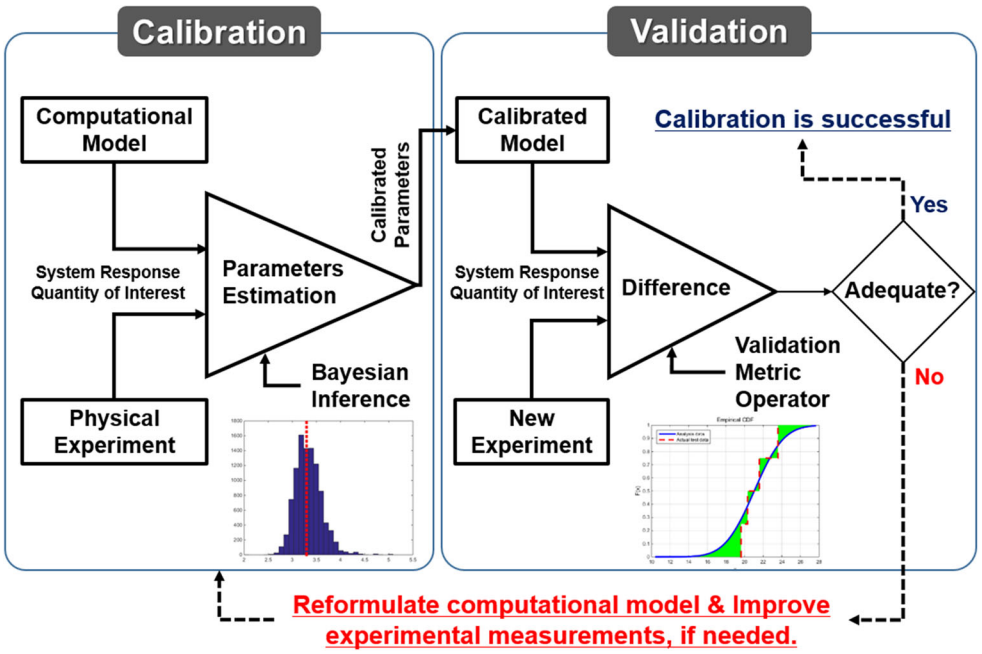

Fig. 2 Overall process of calibration and predictive validation

experimental points by incorporating the correlation between the points. Then the unknown hyper parameters are estimated as a joint posterior distribution using the Bayes' rule. The likelihood of the field data is given by multivariate normal distribution with the mean at the bias added computer model and the covariance function given by the correlation matrix and variance parameters. Once the model is calibrated, it is applied to a new problem, and the predicted distributions are validated by the corresponding new test data. The overall process is illustrated in the Fig. 2 (Oberkampf and Roy 2010). In this study, same statistical approach is employed for the elasto-plastic model of piston insertion into housing in order to obtain close agreement with the actual test data. But, more simple strategy is employed to facilitate practical engineering applications. The original computer model is approximated by the Gaussian process model only in a deterministic sense, which is also known as Kriging surrogate model. The uncertainty due to this approximation is ignored since it is more likely much smaller than the others. Then the calibration process becomes the estimation of the unknown input model parameters, degree of correlation of the bias and the measurement error based on the test data.

The outline of this paper is as follows. In section 2, computational model is addressed that evaluates the resistance force during the piston insertion into the housing, in which the three unknown parameters are identified to be calibrated based on the test data. In section 3, overall process of calibration and validation is carried out, which includes the Kriging surrogate model, calibration of the unknown parameters by Bayesian approach, Markov Chain Monte Carlo (MCMC) simulation to explore their posterior distributions, and predictive validation via new problems and their test data. Conclusions are given in section 4.

2 Computational model

2.1 Computation modeling of piston – housing deformation

Finite element model is constructed with axisymmetric elements to evaluate the piston insertion into the housing with interference, of which the geometry is shown in Fig. 3. The piston is pressed from the top end of housing skirt at point 1 down to the bottom end at point 4, 4.5 mm apart from point 1. The deformation is considered as quasi-static in this model in order to calibrate and validate the axial resistive force obtained from the inert, quasi-static compression test. In ANSYS, PLANE182 with 4 nodes is employed for the solid elements. TARGE169 and CONTA171 are employed for the contact analysis with elasto-plastic deformation under friction. As a result, resistance force of the housing is obtained in terms of the piston displacement from the point 1 to 4 under this assumption.

Since the actual piston diameter may be slightly less than that the inner bore of housing within tolerance limit at initial position (or before actuation), the piston may begin contact with the housing at some distant point 2 in practice, from which the frictional resistance force is created. As the piston proceeds further, it meets protruded part of the housing from point 3, which is made to ensure the piston absorption by the housing and prevent

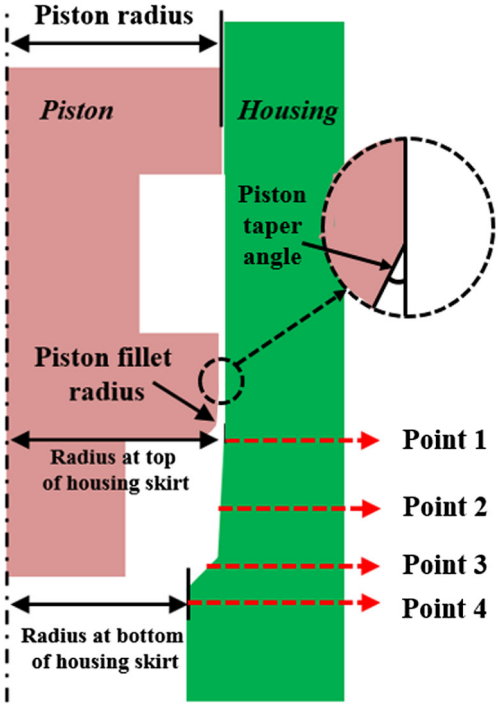

Fig. 3 Axisymmetric geometry model of piston and housing with critical geometry factors affecting the resistance force

bouncing back. An inert, quasi-static compression test result of resistance force in terms of piston displacement is illustrated in Fig. 4.

Materials of the piston and housing are STS630 and STS303, of which the elastic constants are 197 and 195GPa, respectively and Poisson ratio is 0.3 in common. Their measured curves in the form of true strain and true stress are given in Fig. 5. Note that the piston is much stronger than the housing.

2.2 Unknown input parameters

During the analysis, there exist several uncertain parameters that may greatly affect the resulting solutions. First, the friction coefficient μ between the piston and housing is not easily identified because of many factors such as surface condition and magnitude of contact force. Second, since the model is a cutout of interested part of the structure, there is uncertainty for the corresponding boundary conditions, which are at the top end and lower right end of the housing. Fictitious elements are added to account for this, and the finite element model is made as shown in Fig. 6. There may be a number of ways to account for this uncertainty such as introducing equivalent spring elements. In this study, elements with square shape are just added at each boundary as shown in Fig. 6 only to use them as the equivalent spring at the boundary. Then the elastic moduli, E_U and E_L at the additional elements are the unknowns as well. Consequently, the three parameters are treated as the unknowns and estimated based on the test data.

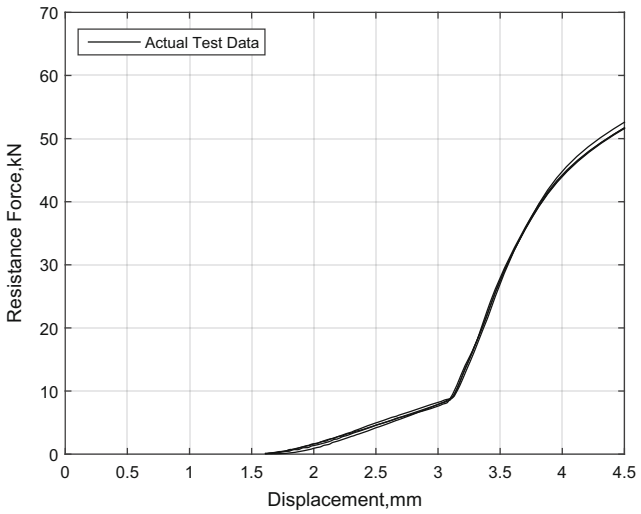

Fig. 4 Typical test result of elasto-plastic insertion

3 Calibration & validation

3.1 Experiments and baseline analyses

Three types of pyro-valves named as A to C are prepared, which differs in dimensions and size but has parametrically same configuration, as shown in the Table 1. Critical geometry factors affecting the resistance force are the radius and fillet radius of the piston, and radius and shape of the skirt of the housing as shown in the Fig. 3. Note that the dimensions are normalized due to the proprietary reasons. Also, the radii profile of the housing from point 1 to 4, which is the critical part in the analysis, is not given by the primitive geometry but by the actual measured data over a finite interval. Due to the machining tolerance, the actual shapes of the housing differ slightly with each other. This actual geometry is accounted for in the analysis model and solution.

Inert, quasi-static compression tests are conducted using an Instron 5582 capable of 100 MN. The upper end of the piston is

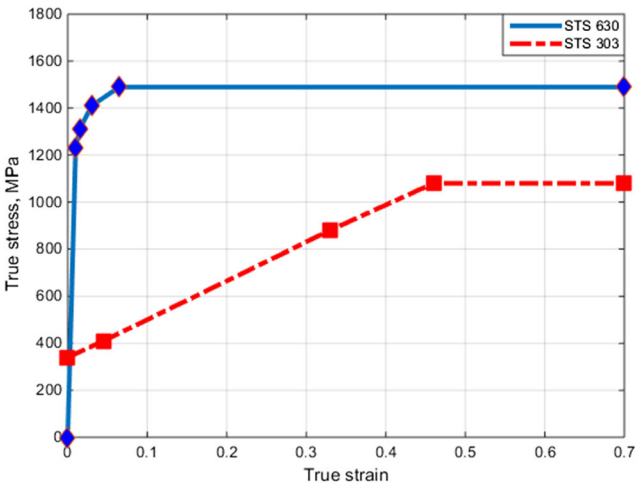

Fig. 5 True stress–strain curve of piston and housing materials

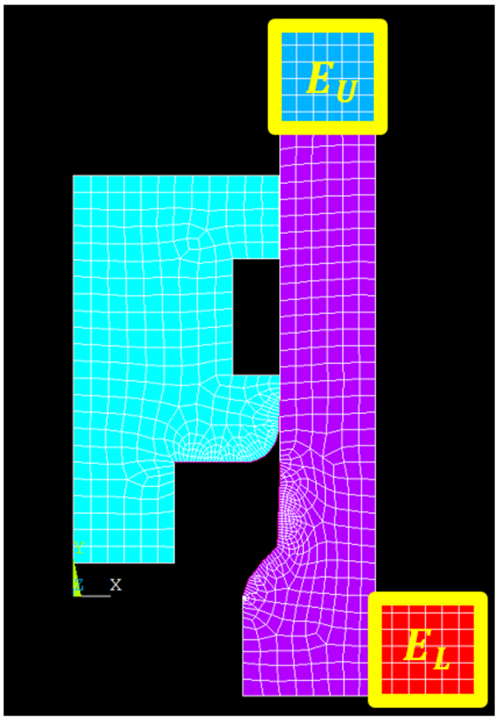

Fig. 6 Finite element modeling of piston and housing with fictitious elements

pushed down by a specially designed cylindrical ram at a constant rate of 2.54 mm/min. The resistance force is recorded as a function of displacement. For each of the types, 5 tests are made. Among the valves, predicted result for the type A is given in the Fig. 7, with the three parameters μ, E_U and E_L set arbitrarily at 0.5, 195GPa respectively. Also, the five test results are superimposed. As expected, the model does not match the test data due to the unknown parameters. The parameters should therefore be calibrated but should account for the uncertainties due to the FE modeling and the variance of test data.

3.2 Kriging surrogate model

When the computation is not trivial as in this FEA which involves contact and plasticity, surrogate model that approximates the original response is usually employed to save the computational cost. Because the original response does not include error in itself, we can construct the

Table 1 Normalized dimensions of five types of pyro-valves

Critical geometry factors	Type A	Type B	Type C
Piston radius	**1.000**	1.141	1.134
Piston fillet radius	**1.000**	1.095	1.857
Piston taper angle	**1.000**	0.500	0.250
Radius at top of housing skirt	**1.000**	1.138	1.132
Radius at bottom of housing skirt	**1.000**	1.270	1.210

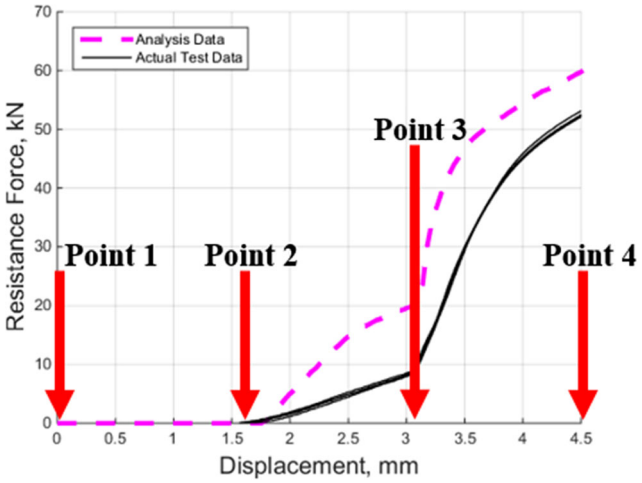

Fig. 7 Comparison of actual test data and analysis result by arbitrary values of three parameters

surrogate model such that it passes the response, i.e., it interpolates the response values. In this study, the Kriging model is constructed in terms of the three unknown input parameters. In order to generate design of experimental (DOE) points in the model, Latin Hypercube Sampling (LHS) method is used. LHS points with $n=25$ are generated including the corner points over the range of three parameters as given in Fig. 8. Kriging model is constructed using the FE analyses results at these points. Since the response is the resistance force as a function of displacement z, the model is constructed at discrete displacement points with equal interval of 0.125 mm in the range 2 ~ 4.5 mm as shown in Fig. 9. Consequently, total of $K=20$ Kriging models are obtained as a function of three parameters

$$\hat{y}(z_k|\mathbf{x}) = \hat{y}(z_k|\mu, E_U, E_L),\ k = 1, \ldots, K \tag{1}$$

where $\mathbf{x}$ are the input parameters μ, E_U and E_L, and z_k is the k'th displacement point, and $\hat{y}$ denotes the Kriging response. At any displacement point, the Kriging model is constructed as a function of $\mathbf{x}$ as follows (Martin and Simpson 2005).

$$\hat{y}(\mathbf{x}) = \mathbf{f}'\beta + \mathbf{r}'\mathbf{R}^{-1}(\mathbf{Y} - \mathbf{F}\beta) \tag{2}$$

where $\mathbf{Y}$ are the FE analysis results at the DOE points of $\mathbf{x}$, which are denoted by $\mathbf{X}$. β and $\mathbf{f}(\mathbf{x})$ are the regression coefficients and trial functions for global approximation, respectively. The matrix $\mathbf{F}$ is the trial function values at these DOE points, i.e., $\mathbf{F}=\mathbf{f}(\mathbf{X})$. The matrix $\mathbf{R}$ denotes the correlation usually defined by a Gaussian type function:

$$\mathbf{R}(\mathbf{x}_i, \mathbf{x}_j) = \exp\left\{-\left(\frac{d}{h}\right)^2\right\},\quad d = \|\mathbf{x}_i - \mathbf{x}_j\|,\quad i, j = 1, \ldots, n \tag{3}$$

where $\mathbf{x}_i, \mathbf{x}_j$ denote the individual DOE points, d is the distance between the two points, and h is an arbitrary

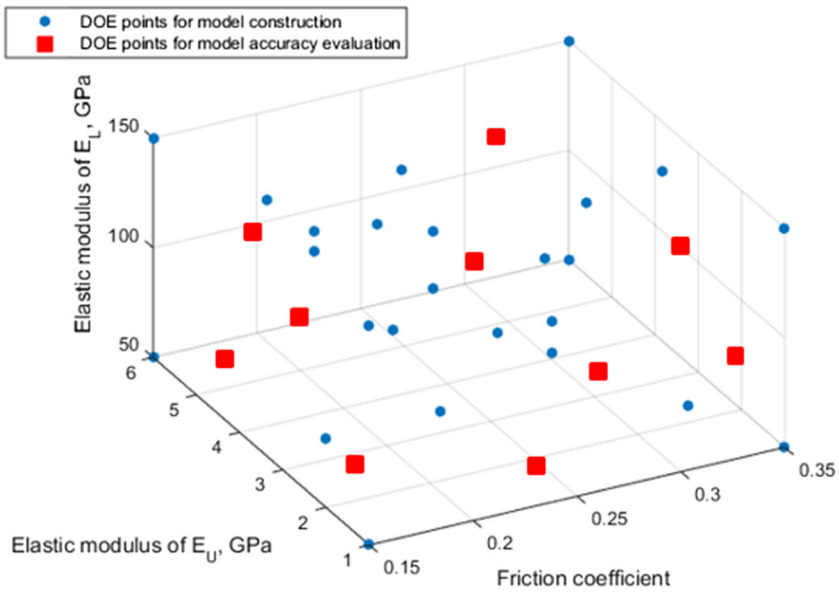

Fig. 8 LHS points over the range of three parameters

correlation parameter which affects the smoothness of the model. Function $\mathbf{r}(\mathbf{x})$ is the correlation between the current point $\mathbf{x}$ and the set of DOE points $\mathbf{X}$, i.e., $\mathbf{r}(\mathbf{x}) = \mathbf{R}(\mathbf{x}, \mathbf{X})$. Note here that $\mathbf{f}$ and $\mathbf{r}$ are the functions of current point $\mathbf{x}$ with the length being the number of trial functions, $\mathbf{Y}$ is the vector with length n, $\mathbf{F}$, $\mathbf{R}$ are the matrices with size n, and β are the constants for $\mathbf{f}$. In this study, constant is employed for the trial function $\mathbf{f}$ and β. The correlation parameter h is 0.01, which is chosen as large as possible such that the approximation is sufficiently smooth but not so large as to cause singularity of $\mathbf{R}$ matrix. In this study, the input $\mathbf{x}$ and the response y denote the three parameters and resistance force at each displacement point given by (1), respectively.

The accuracy of the Kriging model is examined by leaving one out cross validation, in which the prediction error sum of squares (PRESS) and the determination coefficient defined as follows (Myers et al. 2002).

$$R^2_{PRESS} = 1 - \frac{PRESS}{SS_T},$$
$$PRESS = \sum_{i=1}^{n} e^2_{(i,i-1)} = \sum_{i=1}^{n} \left(y_i - \hat{y}_{(i,i-1)}\right)^2, \; SS_T = \sum_{i=1}^{n} \left(y_i - \bar{y}\right)^2 \tag{4}$$

where y_i, $\hat{y}_{i,i-1}$, $PRESS$ and SS_T are the Kriging response with all DOE points included, the Kriging response with one point left out, sum of squares of the leave-one-out cross validation errors and the total variability in the response, respectively. The equation states that if R^2 is close to 1, the accuracy of the model is good. The R^2 values for Kriging model are calculated at every displacement point, from which the minimum is chosen as the accuracy indicator. As a result of calculation for the types A to C, the minimum R^2 is found to be 0.951 for the Kriging model at 5th displacement point of the type C, which indicates favorable accuracy in view of surrogate approximation. The accuracy of the model is further examined by adding 10 new experimental points that are not at the existing DOE points which are generated again by LHS. The points are specified as squares in Fig. 8. In this case, the determination coefficient is defined based on the classical regression as follows.

$$R^2_{regression} = 1 - \frac{SS_E}{SS_T}, \quad SS_E = \sum_{i=1}^{m} \left(y_i - \hat{y}_i\right)^2 \tag{5}$$

where m denotes the number of DOE points for model accuracy evaluation. As a result, the minimum R^2 is found to be 0.959 at 11th displacement point of the type B, better accuracy than the PRESS. Therefore, we can conclude that the error due to the introduction of surrogate model may be negligible and use the Kriging model instead of the original FEA model without uncertainty.

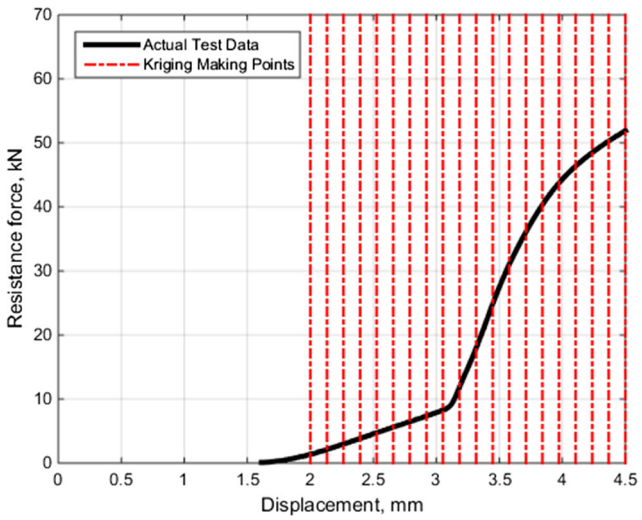

Fig. 9 Kriging surrogate model at points with equal distance

3.3 Calibration and prediction by Bayesian inference

In this section, a procedure for model calibration is addressed based on the Bayesian inference approach in order to account for the associated uncertainties, which is to estimate the unknown input parameters conditional on the test data. The procedure is based on the Bayes' rule as given by Kennedy and O'Hagan (2001), in which the field data are assumed by the combinations of the computer model, bias that incorporates the correlation of the measurements and measurement error:

$$Y(z_k) = \hat{y}(z_k|\mathbf{x}) + b\left(z_k|{\sigma_b}^2\right) + \varepsilon\left(\sigma^2\right),\ k = 1, \ldots, K \tag{6}$$

where Y, $\hat{y}$, b and ε are the observed data, Kriging model, bias (a.k.a. discrepancy term) and measurement error at the k'th displacement point, respectively. Usually the bias is defined by multivariate normal distribution with zero mean as follows (Higdon et al. 2004):

$$b\left(z|{\sigma_b}^2\right) \sim N\left(0, {\sigma_b}^2 Q\right),\ Q = Q(z, z') \tag{7}$$

where ${\sigma_b}^2$ is the variance of the matrix, and Q is the correlation matrix responsible for the smoothness of connection between the two displacement points, usually defined by a Gaussian type function:

$$Q_{ij} = \exp\left(\frac{\left(z_i - z_j\right)^2}{h^2}\right),\quad i, j = 1, \ldots, K \tag{8}$$

As was mentioned in (3), the parameter h is responsible for the degree of smoothness. The value is given as 0.1 for the bias. Note that the bias is introduced to represent the model inadequacy by accounting for the correlation that truly exists between the measurements at the 20 displacement points. Note also that although the assumption of multivariate normal distribution for the bias can be quite restrictive and not necessarily the representative of the other sources of uncertainties, it may not have a significant effect on the resulting calibration and are introduced in several literatures (Kennedy and O'Hagan 2001; Bayarri et al. 2012). Then the bias added computer model may represent the field data more closely by adjusting the gap between the model and field data. The measurement error ε, which represents the uncertainty due to the replication, is assumed to follow the independent and identical normal distribution with the variance σ^2, i.e.,

$$\varepsilon \sim N\left(0, \sigma^2\right) \tag{9}$$

In the Bayesian framework, the unknown parameters are given by the posterior distribution based on the given observation data as follows.

$$P(\mathbf{x}|\mathbf{Y}) \propto L(\mathbf{Y}|\mathbf{x}) P(\mathbf{x}) \tag{10}$$

where $L(\mathbf{Y}|\mathbf{x})$ is the likelihood of observed data $\mathbf{Y}$ conditional on the given parameters $\mathbf{x}$, $P(\mathbf{x})$ is the prior distribution of $\mathbf{x}$, and $P(\mathbf{x}|\mathbf{Y})$ is the posterior distribution of $\mathbf{x}$ conditional on $\mathbf{Y}$. The goal of the Bayesian technique is to improve the knowledge on the unknown parameters $\mathbf{x}$ using the observation $\mathbf{Y}$. As more data are provided, the posterior distribution is used as the prior in the next step and the distribution is updated to more confident information. The procedure to obtain the posterior distribution $P(\mathbf{x}|\mathbf{Y})$ consists of proper definition of the probability distribution for the likelihood and prior. Assuming no prior knowledge for the parameters, the parameters for the posterior PDF of this study consist of the three unknown parameters $\mathbf{x}$ and the two variances ${\sigma_b}^2$ and σ^2. Then the PDF is given by (Gelman et al. 1996)

$$P\left(\mathbf{x}, {\sigma_b}^2, \sigma^2|\mathbf{Y}\right) \propto |R|^{-\frac{1}{2}} \exp\left[-\frac{1}{2}\left\{\mathbf{Y} - \hat{y}(\mathbf{Z}|\mathbf{x})\right\}^T R^{-1}\left\{\mathbf{Y} - \hat{y}(\mathbf{Z}|\mathbf{x})\right\}\right] \tag{11}$$

where

$$R = {\sigma_b}^2 Q + \sigma^2 I \tag{12}$$

In the equation, the symbols $\mathbf{Z}$ and $\mathbf{Y}$ denote the set of displacement points and their corresponding set of observation data, respectively. Since the number of the displacement points K is 20, and number of replications n_r is 5, $\mathbf{Y}$ and $\mathbf{Z}$ consists of 100 data points. The size of matrix $\mathbf{R}$ and $\mathbf{Q}$ are 100×100.

Usually, the posterior PDF of the parameters are determined in the form of samples such that they satisfy (11). This will be addressed in the next section. Once we obtain the samples of the parameters from the posterior PDF based on the existing observed data, we can use this in the prediction of a new analysis problem. In practice, this is to compute the prediction $Y(\tilde{z})$ at a new point $\tilde{z}$ using the following equation (i.e., Gelman et al. 1996)

$$\tilde{Y} = Y\left(\tilde{z}\right) = \hat{y}\left(\tilde{z}|\mathbf{x}\right) + b^p\left(\tilde{z}|{\sigma_b}^2\right) + \varepsilon\left(\sigma^2\right) \tag{13}$$

where

$$b^p\left(\tilde{z}|{\sigma_b}^2\right) \sim N\left(E(b^p), \mathrm{var}(b^p)\right),\quad \begin{array}{l} E(b^p) = {\sigma_b}^2 {Q_1}^T R^{-1}\left(\mathbf{Y} - \hat{y}(\mathbf{Z}|\mathbf{x})\right) \\ \mathrm{var}(b^p) = \left(\tilde{Q} - {\sigma_b}^2 {Q_1}^T R^{-1} Q_1\right){\sigma_b}^2 \end{array} \tag{14}$$

where $\tilde{Q}$ denotes the correlation between the set of new points $\tilde{z}_i$ and $\tilde{z}_j$, and Q_1 is between the new point $\tilde{z}$ and existing set of points $\mathbf{Z}$. Every sample set of the parameters are used to compute the prediction $\tilde{Y}$ in this equation, which in turn constitutes a distribution. Then the upper and lower bounds, which we call the predictive interval (PI) of Y are obtained based on a given confidence level.

In this study, two cases are examined in the calibration process: one is to include the bias which is to account for the model inadequacy by incorporating the correlation of

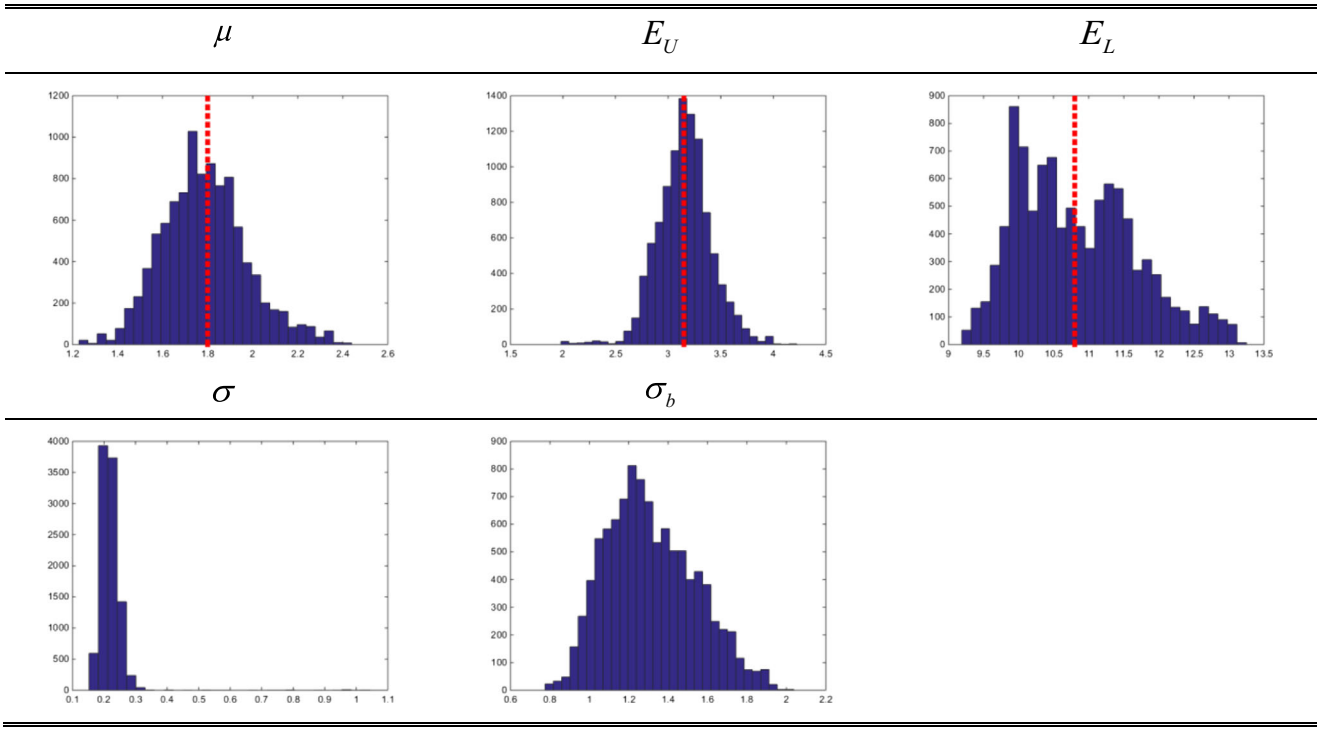

Fig. 10 Result histograms of MCMC simulation for type A and C

the measurements between the displacement points. The other is to ignore the bias, by assuming the computer model truly represents the reality as long as the model parameter values are exact.

3.4 MCMC simulation

Even if the expression of posterior distribution is available as a product of likelihood and prior in (11), the shape of the distribution can only be estimated by calculating its values at different points. A primitive way is to compute the values of PDF at a grid of points after identifying the effective range and to calculate the value of the posterior distribution at each grid point. This method, however, has several drawbacks, such as the difficulty in selecting the location, spacing, and scale of the grid points. In addition, it becomes computationally expensive when the number of updating parameters increases. MCMC simulation is a computationally effective alternative which generates a chain of samples to plot the PDF. The Metropolis–Hastings algorithm is a common choice for MCMC simulation; it is summarized in (15).

$$
\begin{aligned}
&1.\ \text{Initialize } \mathbf{x}^{(0)}\\
&2.\ \text{For } i = 0 \text{ to } N-1\\
&\quad -\text{Sample } u \sim U(0,1)\\
&\quad -\text{Sample } \mathbf{x}^{*} \sim q\left(\mathbf{x}^{*}|\mathbf{x}^{(i)}\right)\\
&\quad -\text{If } u < \min\left\{1,\ \frac{P(\mathbf{x}^{*})q(\mathbf{x}^{(i)}|\mathbf{x}^{*})}{P(\mathbf{x}^{(i)})q(\mathbf{x}^{*}|\mathbf{x}^{(i)})}\right\},\\
&\qquad\quad \mathbf{x}^{(i+1)} = \mathbf{x}^{*}\\
&\quad -\text{else}\\
&\qquad\quad \mathbf{x}^{(i+1)} = \mathbf{x}^{(i)}
\end{aligned}
\tag{15}
$$

Table 2 Sample statistics of MCMC simulation and deterministic optimum for types A ~ C

Type	μ			E_U (GPa)			E_L (GPa)		
	Mean	Optimum	95 % PI	Mean	Optimum	95 % PI	Mean	Optimum	95 % PI
A	0.178	0.168	[0.145, 0.221]	3.162	3.302	[2.707, 3.669]	108.428	116.665	[95.336, 127.403]
B	0.175	0.178	[0.129, 0.233]	3.289	3.449	[2.695 3.881]	113.795	112.353	[98.905, 129.536]
C	0.164	0.162	[0.149, 0.236]	3.644	3.296	[2.682, 3.909]	85.020	119.499	[64.318, 116.960]

Table 3 Sensitivity study results for the group 1

Type	RMSE	Sensitivity (%)		
		μ	E_U	E_L
A	1.42	21	23	6
B	1.09	32	25	8
C	1.86	27	29	13

For convenience of notation, the symbol **x** in this equation is defined to include all the parameters in the posterior PDF in (11), i.e., the three unknown parameters **x** and the variances σ_b^2 and σ^2. $\mathbf{x}^{(0)}$ are the initial values of the parameters to be estimated, N is the number of iterations or samples, $U(0,1)$ is the uniform distribution in the interval of [0,1], $P(\mathbf{x})$ is the posterior distribution, and $q(\mathbf{x}^*|\mathbf{x}^{(i)})$ is an arbitrarily chosen proposal distribution. Uniform or Gaussian distribution at the current point with finite length or scale are the normally chosen. A uniform distribution is used in this study for the sake of simplicity. Then, $\mathbf{x}^*$ becomes a uniform distribution centered at $\mathbf{x}^{(i)}$ with the interval of $\pm w$, where w is a vector for setting the sampling interval. If the sample $\mathbf{x}^*$ is not accepted as an $(i+1)^{\text{th}}$ sample, the i^{th} sample becomes the $(i+1)^{\text{th}}$ sample; that is, the particular sample is doubly counted.

3.5 Result of MCMC simulation

MCMC simulation is carried out to obtain the posterior distributions of three parameters and the two variances based on the test data. The resulting histograms of the estimated parameters are given with 10,000 samples for the types A in Fig. 10. The distributions reflect the uncertainties of the parameters that are caused by the model and measurement errors. In the Fig. 10, the values by deterministic optimization are given as well by the dotted line, which are obtained by minimizing the root mean square errors (RMSE) between the model and test data, i.e.,

$$\min_{\mathbf{x}} RMSE = \sqrt{\frac{1}{n_r K}\sum_{k=1}^{K}\sum_{i=1}^{n_r}\left(y_i^k - \hat{y}(z_k|\mathbf{x})\right)^2} \tag{16}$$

Table 4 Correlation value between the three parameters for types A ~ C

Type	μ & E_U	μ & E_L	E_U & E_L
A	−0.7319	−0.1895	0.1705
B	−0.7853	−0.2047	0.2139
C	−0.6199	−0.2451	0.1774
Mean	**−0.7124**	**−0.2131**	**0.1873**

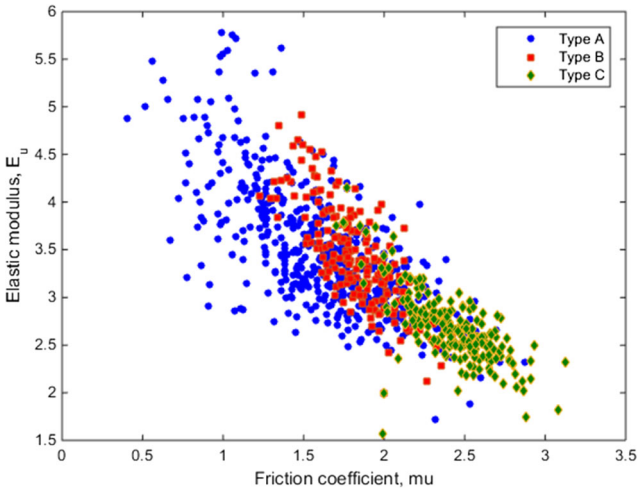

Fig. 11 Correlation plot of μ and E_U

The sample statistics are also found in the Table 2, in which the mean, 95 % predictive interval (PI) and deterministic optimum of the parameters are given for all three type models.

From the results, following observations are made. First, the distributions enclose the deterministic optimum at close to their means, which means that by using the distribution solutions, we can obtain not only the point estimations but also their uncertainties in the form of confidence limits. Second, while the distributions of the other parameters are well behaved, i.e., narrow and relatively sharp, that of E_L is not good. This is because the contribution of E_L to the response is much smaller than the others. This is evidenced by the sensitivity study of the resistance force with respect to the three parameters. Using the standard deviations obtained from each distributions, the percentages of RMSE variation are calculated by varying each of the parameters by 2 standard deviations and results are given in Table 3 for the group 1. It is found that E_L affects the resistance force much less than the other two, which means that the estimated distribution can be wider and ill-behaved than the others. Third, the calibrated solutions for the two parameters μ and E_U from each of the types A ~ C are different each other as can be seen in the Table 2 (means of μ and E_U vary in the range 0.164 ~ 0.175 and 3.13 ~ 3.60GPa, respectively, which are not small), which states that the solution for μ and E_U may not be unique. The reason may be attributed to the correlation between the two parameters. This is evidenced by the correlation values between the three parameters, which is given in Table 4 for the types A ~ C. High correlations are found between μ and E_U as opposed to the other two. The high correlation can also be seen by drawing the sample points of MCMC simulation in Fig. 11. Due to this nature, there may be no unique solution for

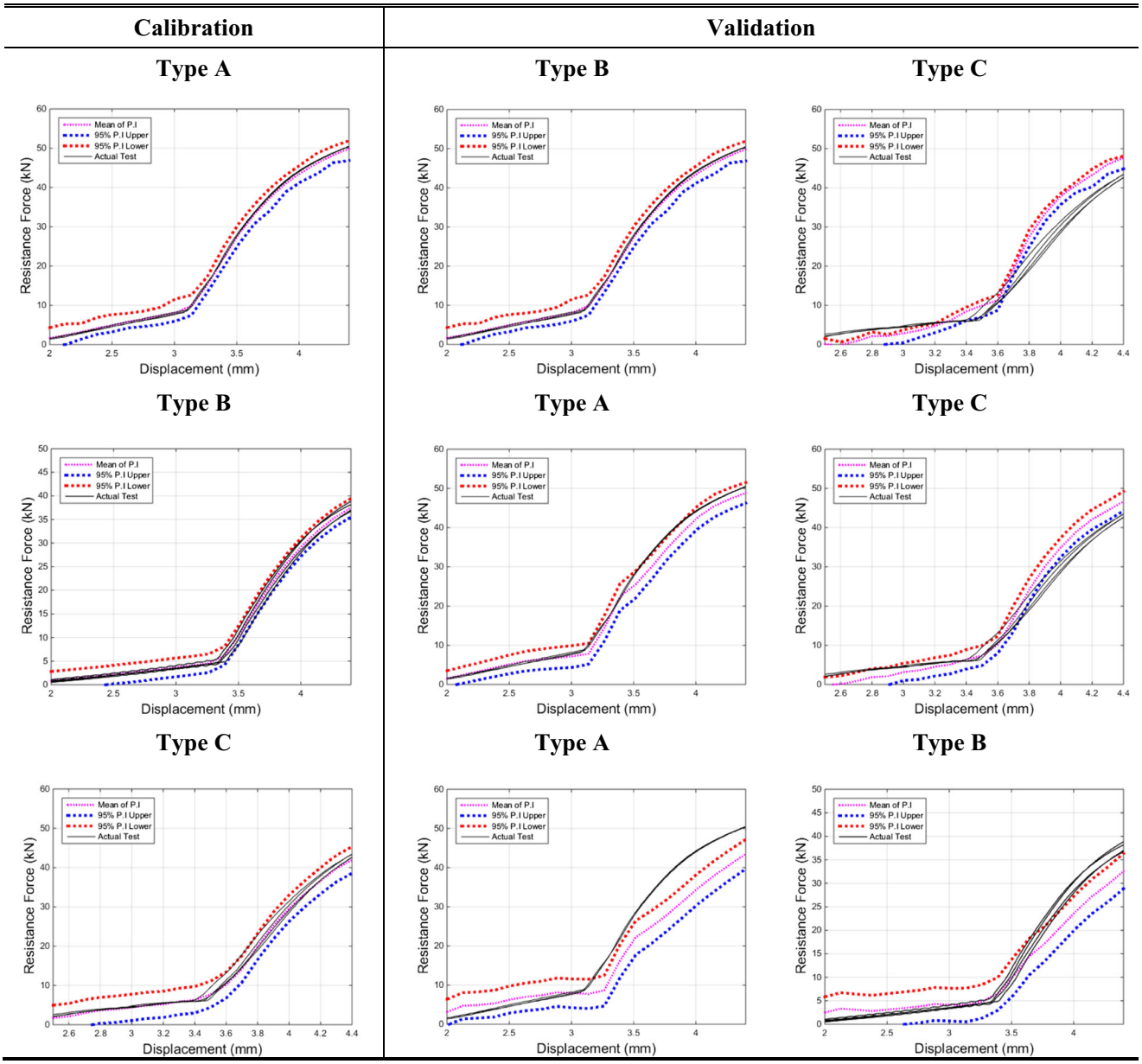

Fig. 12 Cross validation of three types A ~ C by comparing the predictive interval and test data: result with bias

the two parameters, and the solution may be different every time we calibrate. Nevertheless, the predictive distribution is the same regardless of this difference, as can be found in the next section.

The above results are those including the bias and its associated variance σ_b^2 that reflects the correlation of measurements between the displacement points. We can also go through the same process by ignoring this, which is to determine the posterior distributions of the three parameters and the variance σ^2 of the measurement error only. The resulting distributions are almost the same as those with σ_b^2, hence, are not presented here.

3.6 Validation of the prediction

In order to validate that the calibrated model is useful, the predicted distribution should be made for a couple of new problems and compared with their test data. For this purpose, cross validation is carried out, in which the parameters calibrated by the types A to C are applied one at a time to obtain the predicted distributions of the other two types. Then the results are validated by comparing the PI of the resistance force and test data together. If all the test data are enclosed within the PI, the model is regarded as valid and useful in the new problem.

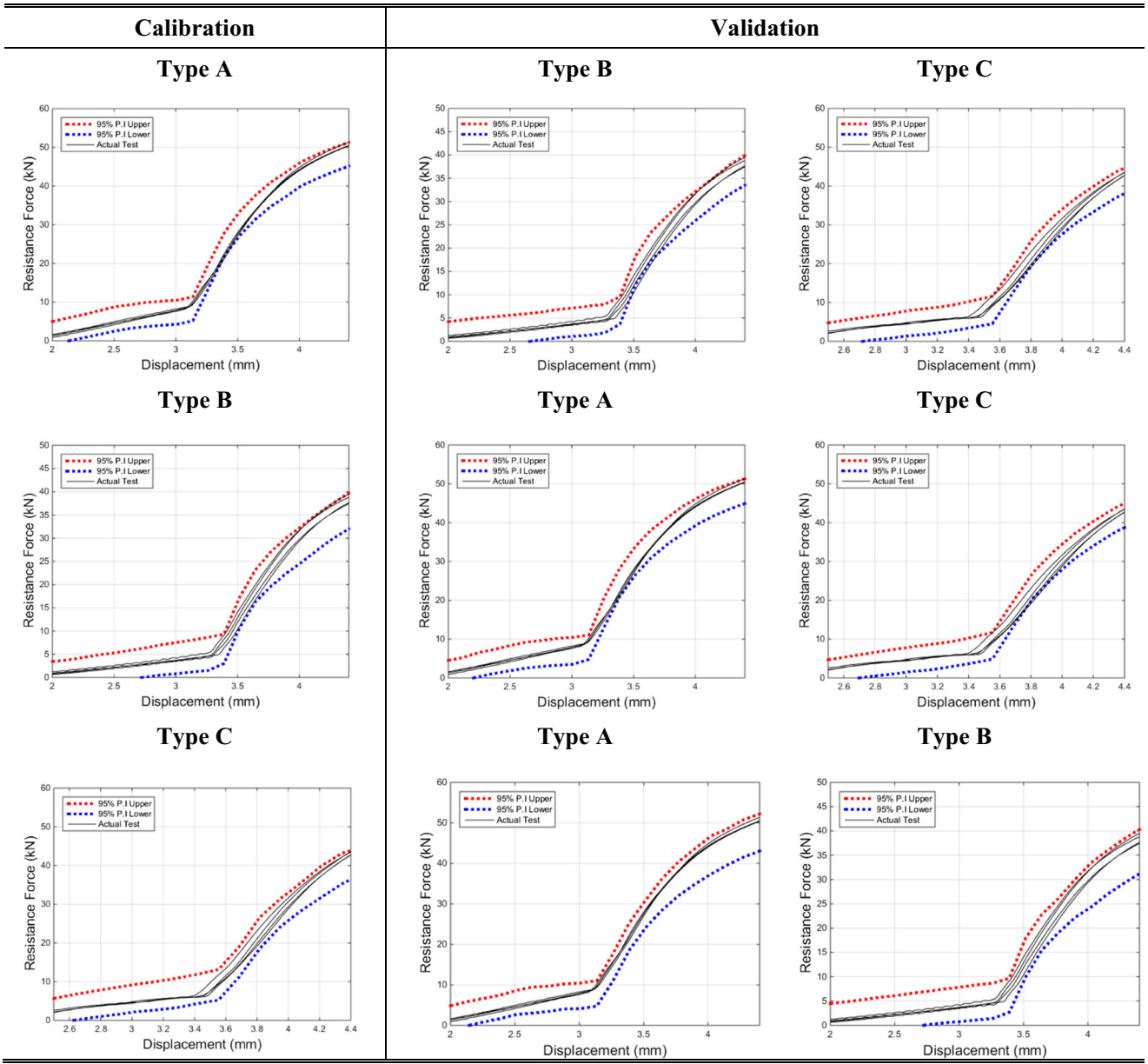

Fig. 13 Cross validation of three types A ~ C by comparing the predictive interval and test data: result without bias

In Fig. 12, the PIs and test data for the three type models are plotted. The most left figures are the predictive distribution for the calibrated model, whereas the right two are those for the other two models. As expected, it is obvious that all the PIs for the calibrated model enclose the test data very closely with narrow widths because the predictions are made for the same model, and include the correction of the bias that represents the discrepancy between the test data and model. Applying the calibrated parameters to the other two types, however, the PIs of the predictions do not enclose the data well. The reason is due to the application of bias that was used to match with the test data of the calibrated model into the different models. This can be explained by (14) in which the **Y** denotes the test data made for the calibration model, not for the new validation model. Therefore, the approach including the bias that considers the correlation of measurements between the displacement points is not recommended. On the other hand, the PIs and test data by ignoring the bias and correlation are plotted in Fig. 13. The PIs of the predictions to the other two types enclose the test data successfully, although the PI widths are wider than those with the bias.

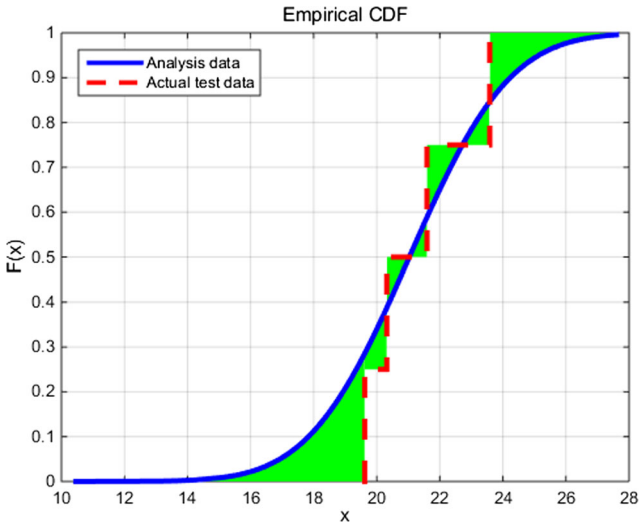

Fig. 14 CDF area difference between test data and predictive distribution data

Nevertheless, the model calibration is valid and useful for the new models without having to run the test for validation. From these findings, it is acknowledged that the uncertainty of the model error cannot be explicitly considered but only incorporated within the measurement error.

In the validation, area metric given by the CDF difference which is introduced in (Ferson et al. 2008) is also a good measure due to the advantage of quantitative evaluation. The concept is illustrated in Fig. 14, and defined as follows.

$$A_d = d(F, S_n) = \int_{-\infty}^{\infty} |F(x) - S_n(x)| dx \tag{17}$$

where y is the resistance force, and F and S_n denote its CDF by predictive distribution and multiple tests, respectively. Since we have 20 displacement points and response values, the maximum area metrics is chosen for the validation. The results are given in Table 5, in which the area metric from the calibrated model is used as the reference and the ratio of the other two of the predictive validation are used as a relative measure of validation accuracy. If the values are similar or greater by small value in the other two predictions, the ratio is close to 1 and, the model is regarded as successfully validated, and is allowed to use for the next new case.

Table 5 Comparison of the normalized maximum area metrics for types A ~ C

	Type A	Type B	Type C
Type A	**1.000**	1.030	1.165
Type B	1.197	**1.000**	1.219
Type C	1.511	1.068	**1.000**

4 Conclusions and discussions

In this work, a statistical method for calibration and validation is proposed to develop a reliable computational model that is close to the test data. The method is applied to the problem of piston insertion into the housing in the pyro-valve device. Computational model is developed to carry out elastoplastic and contact analysis during the piston movement into the housing. Surrogate model is developed to save computational time, which is a function of three unknown parameters that are to be calibrated based on the test data. By employing Bayesian approach and Markov Chain Monte Carlo (MCMC) simulation, the posterior distributions of the unknown parameters are estimated efficiently. In order to examine that the calibrated model hold true in the similar new analyses, additional problems are introduced, analyzed and tested for validation purpose. Several observations are found in this study.

First, there may be some correlated nature between the unknown parameters as in the case of μ and E_U in this study. The prediction in the new problem, however, works equally well although we are not able to find out unique parameters.

Second, some parameters may exhibit ill-conditioned distribution such as E_L in this study. This is due to the lower contribution of the parameter to the response, and may be of little concern.

Third, the introduction of bias and correlation in the calibration may lead to overfitting problem that may match closely the test data for the calibration model but may not be the case for the different models. In order to avoid this, it is suggested to ignore the bias and correlation in the calibration, and estimate the unknown input parameters and variance of the measurement error only, although the PI widths may be wider to some degree than those with the bias. In some sense, this is counterintuitive in that the addition of correlation of the measurement error as the bias in the calibration does not provide better accuracy of calibration. The reasons may be attributed to: (1) other sources of uncertainties (e.g. other model parameters than the ones considered in this study) that were not explicitly considered may have effect on the calibration. (2) the correlation model for the bias may not have appropriately represented the problem.

As a conclusion, the method is found useful and validity of the model is ensured, which suggests its use in the subsequent new design with similar configuration. There are still limitations in this approach, which is the problem of to what extent the developed model is valid. There is no quantitative guideline and this should be the topic of future study. Nevertheless, as long as the new design remains in the same parametric configuration, the method can be worth applying for the sake of time and cost.

Acknowledgements This work was supported by the agency for defense development under the grant "International collaborative research program", which is greatly appreciated.

References

Bayarri MJ, Berger JO, Paulo R, Sacks J, Cafeo JA, Cavendish J, Lin CH, Tu J (2012) A framework for validation of computer models. Technometrics 49(2):138–154

Braud AM, Gonthier KA, Decroix DE (2007) System modeling of explosively actuated valves. J Propuls Power 23(5):1080–1095

Ferson S, Oberkampf WL, Ginzburg L (2008) Model validation and predictive capability for the thermal challenge problem. Comput Methods Appl Mech Eng 197(29):2408–2430

Gang JH, An DW, Joo JW, Choi JH (2012) Uncertainty analysis of solder alloy material parameters estimation based on model calibration method. Microelectron Reliab 52(6):1128–1137

Gelman A, Meng XL, Stern H (1996) Posterior predictive assessment of model fitness via realized discrepancies. Stat Sin 6(4):733–760

Higdon D, Kennedy M, Cavendish JC, Cafeo JA, Ryne RD (2004) Combining field data and computer simulations for calibration and prediction. SIAM J Sci Comput 26(2):448–466

Jones BK, Emery AF, Hardwick MF, Ng R (1994) Analysis of explosively actuated valves. J Mech Des 116(3):809–815

Kennedy MC, O'Hagan A (2001) Bayesian calibration of computer models. J R Stat Soc 63(3):425–464

Martin JD, Simpson TW (2005) Use of Kriging models to approximate deterministic computer models. AIAA J 43(4):853–863

Marwala T, Mdlazi L, Sibusiso S (2005) Finite element model updating using Bayesian framework and modal properties. J Aircr 42(1):275–278

Myers RH, Montgomery DC, Anderson-cook CM (2002) Response surface methodology process and product optimization using designed experiments. Wiley, New York

Oberkampf WL, Roy CJ (2010) Verification and validation in scientific computing. Cambridge University Press, Cambridge

Paul BH, Gonthier KA (2010) Analysis of Gas-dynamic effects in explosively actuated valves. J Propuls Power 26(3):479–496

Sankararaman S, Ling Y, Mahadevan S (2011) Uncertainty quantification and model validation of fatigue crack growth prediction. Eng Fract Mech 78(7):1487–1504

Simpson TW, Mauery TM, Korte JJ, Mistree F (2001) Kriging models for global approximation in simulation-based multidisciplinary design optimization. AIAA J 39(12):2233–2241

Straub D, Papaioannou I (2014) Bayesian updating with structural reliability methods. J Eng Mech 141(3):04014134

White MD, Jones N (1999) Experimental quasi-static axial crushing of Top-hat and double-hat thin-walled sections. Int J Mech Sci 41(2):179–208